The Fourth Engineering Conference
"Renewable Energies and Confronting Climate Change to Achieve Sustainable Development" 12-13/12/2023

DESIGN AND IMPLEMENTATION OF THREE-PHASE PV INVERTER OF SiC-IGBT SWITCHES FOR GRID SYNCHRONIZATION WITH PV STATIONS

Ibrahim Abdelkarim. Saad. Abdelkader [1*],
[1] mgily80@gmail.com
*Corresponding mgily80@gmail.com

ABSTRACT

The PV inverters used to integrate the utility grid-connected with PV power systems are typically produced using silicon insulated gate bipolar transistors (Si. IGBT). The efficiency of Traditional PV Inverter (TPVI) can be enhanced by substituting the current Si IGBT switches with silicon Carbide insulated-gate bipolar transistor (SiC. IGBT), due to the physical limitations of of silicon transistors. With the conducted experimental testing, the primary objective of this study was to show that an increase in efficiency was achievable when SiC-IGBTs were employed in TPVI systems. A secondary objective was to provide international rules and grid synchronization with PV systems. In this paper, two experimental setups were explored for this aim., double pulse test (DPT) using SiC.IGBT and Si.IGBT and TPVI based Si-IGBT. The DPT and TPVI were developed and created in order to compare both switches. The TPVI based on SiC.IGBT will be tested in the next study. The turning on and turning off processes were investigated, and the findings were given. Experimentally, silicon.IGBT efficiency in the DPT measured at 77%, whereas SiC.IGBT efficiency in DPT was increased to 95%. The TPVI system based on Si-IGBT is 86% efficient. The increase in efficiency that would result from employing SiC-IGBTs in TPVI.
Keywords: silicon Photovoltaic inverters; SiC.IGBT; Si.IGBT; high-speed switching; International regulations.

تصميم وتنفيذ عاكس كهروضوئي ثلاثي الطور مكون من ترانستور نوع سليكون كاربا يد لمزامنة الشبكة العامة للكهرباء مع محطات الخلايا الشمسية

إبراهيم عبدالكريم سعد عبدالقادر *

mgily80@gmail.com

*Corresponding mgily80@gmail.com

الخلاصة

العاكس الكهربائي أو المحول ((Inverter) الذى يتم استخدامه في ربط شبكة الكهرباء العامة مع أنظمة الطاقة الكهروضوئية يتكون من ترانزستور مصنوع من مادة سيليكون (Si-IGBT). يمكن تحسين كفاءة العاكس الكهروضوئي التقليدي باستبداله بنوع اخر مكون من ترانزستور مصنوع من كربيد السيليكون (SiC-IGBT). من خلال التجارب العملية التي تم إجراؤها والتي أوضحت تحقيق الهدف لأول من هذه الدراسة والمتمثل في تحسين الكفاءة عند استخدام (SiC-IGBT) في العاكس التقليدي المصنوع من (Si-IGBT). الهدف الثانى من هذه الدراسة هو بيان القواعد والقوانيين الدولية المطلوبة الاعتماد عليها عند ربط الشبكة العامة للكهرباء ومزامنتها مع المحطات الكهروضوئية. لغرض تحقيق اهداف هذه الدراسة تم اجراء تجربتان , التجربة الأولى هي استخدام النبض المزدوج (DPT) المعتمد على (Si-IGBT) وكذلك (SiC-IGBT) , بينما التجربة الثانية تم استخدام العاكس التقليدي المعتمد فقط على (Si-IGBT). تم تطوير وإنشاء النبض المزدوج (DPT) والعاكس التقليدي لغرض المقارنة بينهما. سيتم اختبار العاكس التقليدي المعتمد على (SiC-IGBT) في البحث والدراسة الجديدة. تم اجراء عمليات التشغيل (turning on) والإيقاف (turning off) عدة مرات وتم الحصول على النتائج . عمليا وبالتجارب ، تم قياس كفاءة (Si-IGBT) في النبض المزدوج (DPT) والكفاءة كانت بنسبة 77% ، في حين تمت زيادة (SiC-IGBT) في النبض المزدوج (DPT) والكفاءة زادت بنسبة 95.%. نظام العاكس التقليدي المعتمد على (Si-IGBT) كانت النسبة 86%. الزيادة في الكفاءة قد نحصل عليها عند استخدام نظام العاكس التقليدي المعتمد على (SiC-IGBT) .

الكلمات المفتاحية :

العاكس السيليكون الضوئي (Si-Photovoltaic inverter), كربيد السيليكون (SiC-IGBT) , السيليكون (Si-IGBT) , مفاتيح ذات سرعة عالية (high-speed switching) , اللوائح والقوانيين الدولية (International regulations).

1. Introduction

Traditional silicon Photovoltaic inverter (TPVI) are used to connect with electrical grid to supply the required electricity. The main disadvantage of silicon switches is their lower switching frequency which results in an increase in the volume, weight, and passive components [1]. The Si.IGBTs is an appropriate transistor for high power applications because it combines the high input impedance of a MOSFET with the high current density of a bipolar device [2,3]. Due to its acceptable weight, faster switching rates, and lower voltage drop, SiC. IGBT devices can replace Si-IGBT devices in order to increase the effectiveness of the new TPVI[4-6]. The first goal of this study was to show that an increase in efficiency could result in the case of using silicon carbide insulated gate bipolar transistor (SiC.IGBTs) in TPVI systems with the actualized experimental tests while the second goal was international regulations and grid synchronization with PV will be presented. The PV inverter need to disconnect from the grid in case of abnormal grid conditions in terms of voltage deviations and frequency deviations. In several articles, the flipping properties of SiC transistors and those of their Si counterparts were compared.

Several papers compared the SiC transistors and their Si counterparts. According to Kadavelugu and Wang [7,8], the SiC material's bigger band gap, stronger breakdown field, and greater temperature stability are the reasons why the SiC-IGBT behaves quite differently from the Si-IGBT. According to [9]. Due to their smaller drift area, SiC.IGBTs have a lower equivalent on resistance than Si.IGBTs at the same rated voltage. Previous research has shown that compared to equivalent Si.IGBT transistors, SiC.IGBT power devices may perform better performance. However, a survey of the literature showed that SiC.IGBT was not applied to TPVIs.

The double-pulse test (DPT) using Si-IGBT and SiC-IGBT will be used and explored in this article; the TPVI-based Si-IGBT will be used and investigated in the this article while the TPVI-based SiC-IGBT will investigated in the next article. The evaluation of two experimental systems was provided. A DPT system based on Si.IGBT and SiC.IGBT was developed for the initial experiment. A TPVI using Si.IGBT switches was developed for the second trial. SiC.IGBT and Si.IGBT device characteristics were compared and studied under RL loads. The effects of turning on and turning off are measured and explained in more detail. Experimentally, the Si.IGBT with a DPT had an efficiency of 77%, whereas the DPT with a SiC.IGBT had an efficiency of up to 95%. The Si.IGBT-based TPVI system has an 86% efficiency. The experiments ' findings showed that the SiC.IGBT had a lower loss than the Si.IGBT and a faster switching speed. In order to choose the type of IGBT modules in line with the requirements of the TPVI application, the suitable technical basis has to be built.

The rest of the text is structured as follows: Grid requirements for PV, grid synchronization, and islanding detection are discussed in Section 2. Section 3 presents the inverters' design and design considerations. Section 4 displays the test systems and experimental circuits. The final two sections are the debate in Section 5 and the conclusion in Section 6.

2 . PV inverter Topology

The PV inverter, which is an main component of grid-connected PV power systems, transforms the DC power produced by PV panels into grid-synchronized AC electricity. Figure 1 shows the topology of PV inverter. It could be challenging to increase the efficiency with this technology. In this study, a highly efficient microcontroller control circuit was used to create the PWM signals. These signals will control the IGBTs' switching behavior during the conversion of direct current (DC) to alternate current(AC) as pure signals [10,11]. The control mechanism of the TPVI system used temperature and current sensors (ACS712) to each phase leg.

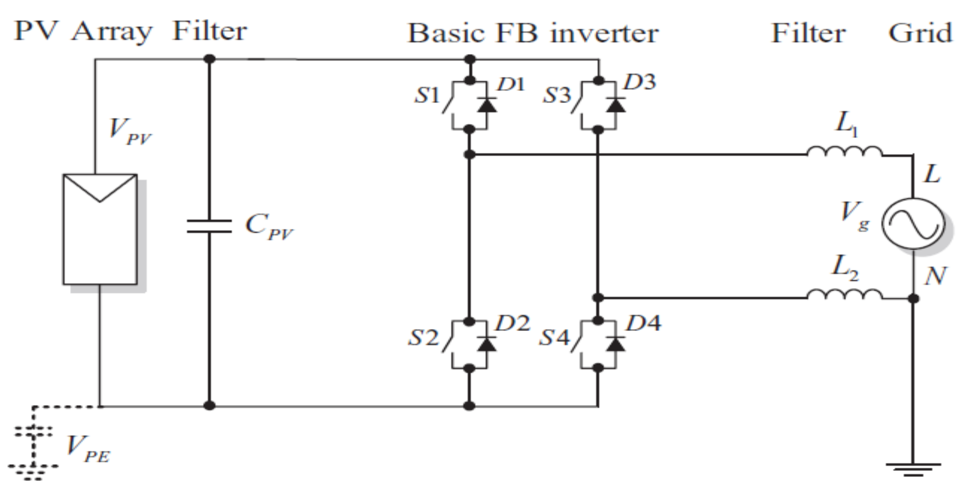

Figure 1. PV inverter Topology[12].

2.1. Grid Requirements for PV circuit.

Grid disconnection can occur as a result of a local equipment failure detected by ground fault protection. When there are abnormal voltage and frequency conditions on the grid, the PV inverters must be disconnected. As shown in table 1 the required disconnection time for VDE 0126-1-1 is much shorter (0.2 sec.).The fast voltage monitoring is thus required and the time delay in IEC 61727 is an extra measure to ensure resynchronization before reconnection in order to avoid possible damage. The grid specifications are important requirement that has a significant influence on the design and functionality of the PV inverter[12]. Table 1 shows the international grid regulations.

Table .1 International Regulations [12].

	Descriptions	**Name**
1	IEEE 1547 Interconnection of Distributed Generation	*Focuses on all types PV systems up to 10 MW. * Focuses on the technical specifications and testing. * There are general specifications, responses to abnormal conditions, power quality, islanding, and test specifications.
2	IEC 61727 Characteristics of Utility Interface	*Specifies the conditions for connecting PV systems to the utility distribution grid. * Applicable to PV power systems with utility connections that run in parallel with the utility grid to convert DC to AC.
3	VDE 0126-1-1 Safety	* The PV inverter will automatically be disconnected from the grid in situations including, fault current, and inadequate earth isolation,. * Automatic disconnection device between a PV power systems and the public low-voltage of the utility grid .
4	IEC 61000 Electromagnetic Compatibility	*Focuses on limiting the injection of harmonic currents into the public supply utility grid system.
5	EN 50160 Public Distribution Voltage Quality	*Outlines the main voltage characteristics and their permitted deviation ranges at the point of common coupling with the customer in public low-voltage of the utility grid under standard operating conditions
6	Corresponding standard IEC 61000-3-3	* Limiting flicker and voltage fluctuations is an issue. * impressed on public low-voltage of the utility grid.

2.2.Grid Synchronization in Power Converters

Monitoring of the utility grid variables is a necessary task to be implemented in the power converter interfacing PV power systems to the grid. The grid codes state the voltage and frequency boundaries within which the PV power systems should remain connected to the utility grid while ensuring stable operation. Hence, the power converter of these PV power systems should accurately screen the utility grid variables at the point of common coupling (PCC) in order to trip the disconnection procedure when they go beyond the limits set by the grid codes. Grid monitoring and grid synchronization are two closely linked concepts. Grid synchronization is a fundamental issue in the connection of power converters to the utility grid since it allows the grid and the synchronized power converter to work in unison.

The information about the phase-angle of the grid voltage is necessary to transform the grid variables from the natural reference frame to the synchronous reference frame, which makes it possible to deal with DC variables in the regulation of AC voltages or currents supplied to the utility grid by the power converter. The grid synchronization techniques used in power systems can be classified into two main groups, namely the frequency-domain and the time-domain detection methods. The frequency-domain detection methods are usually based on some discrete implementation of the Fourier analysis. The time-domain detection methods are based on some kind of adaptive loop such as phase-locked loop (PLL) [12].

2.3. Islanding Detection

The grid-resident methods are based on the communication between the grid and PV inverters and are completely different from the other inverter-resident techniques. In fact, a transmitter (T) is installed near the line protection switch and a receiver (R) is positioned in the PCC in the proximity of the inverter. Under normal conditions of operation a specific frequency signal is sent to the receiver using the energized power lines. The same goal can be achieved with a dedicated line of communication. This method is very good for islanding detection because it is independent from power flows. The evolution of grid resident methods could be done using a supervisory control and data acquisition system (SCADA) even if the penetration of this communication systems in the low voltage distribution grid is limited to smart metering [13].

3. Considerations and design

In this chapter, the key practical considerations for setting up an inverter lab setup and design of gate drivers are shown below:

3.1. Gate Driver Requirements

To simultaneously control the top and bottom transistors, the gate driver circuit board uses two different gate drivers. The gate drive's design considerations have been previously documented [14]. Through the IGBT drivers, the snubber capacitor's extremely quick charge/discharge switching rate will control the gates for the transistors. The top and lower gate drivers of the actual built circuit are shown in Figure 2. The input capacitance must thus be charged with a greater gate current, When the IGBT is off, the same current capability is needed. It is possible to increase the gate current capacity by reducing the gate resistors for external turn off and turn on. To obtain a quick and safe turn-off transient, SiC.IGBT need a negative gate to emitter voltage similar to that seen in Si-IGBTs. A SiC-IGBT driver generally supplies a gate-to-emitter voltage of +20 V positive and - 5V negative[15]. The power circuit and the control circuit are isolated from one another using galvanic isolation. The top and bottom transistors in the half bridge circuit are driven by two different gate drivers[16].

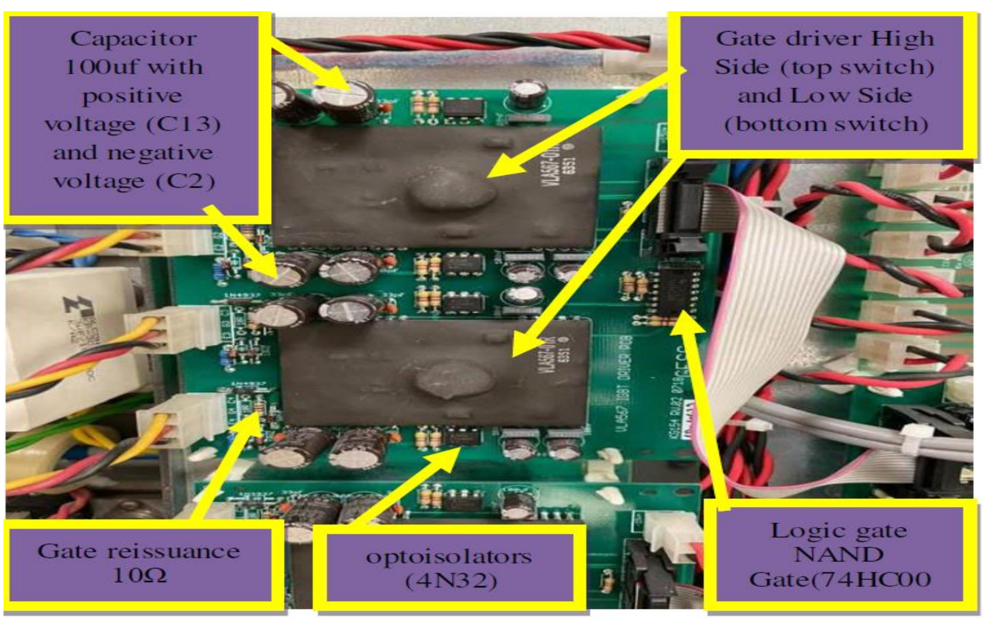

Figure 2.Diagram of implemented circuit gate drive .

4. Experiments

In this section, two experiments are presented. Three Phase PV Inverter (TPVI) and Double Pulse Test (DPT) were the two experiments, respectively. The processes for turning on and off the two IGBT switches were evaluated under RL loads, and the findings were presented.

4.1. Double Pulse Test Experiment

In this part, two experiments are performed. In the first experiment, Si-IGBT switches based on the DPT were evaluated, and in the second experiment, SiC.IGBTs based on the DPT were also evaluated. Utilizing a single Si.IGBT (CM150DY-24A) and a single SiC IGBT (SK25GH063) switch, experimental monitoring of the switch-on and switch off waveforms of the upper and lower switch has been conducted under RL load (R = 42 ohm, L = 290 uH).Use the DPT to study Si-IGBT and SiC-IGBT hard-switching transient that turns on the upper transistor on higher side (rising edge) and turns off lower transistor on the lower side (falling edge). The top switch will be activated with a positive gate voltage and charge a current through the load during the initial pulse, whereas the bottom switch will be deactivated with a negative gate voltage [17]. Figure 3 shows the circuit used to create the both switches.

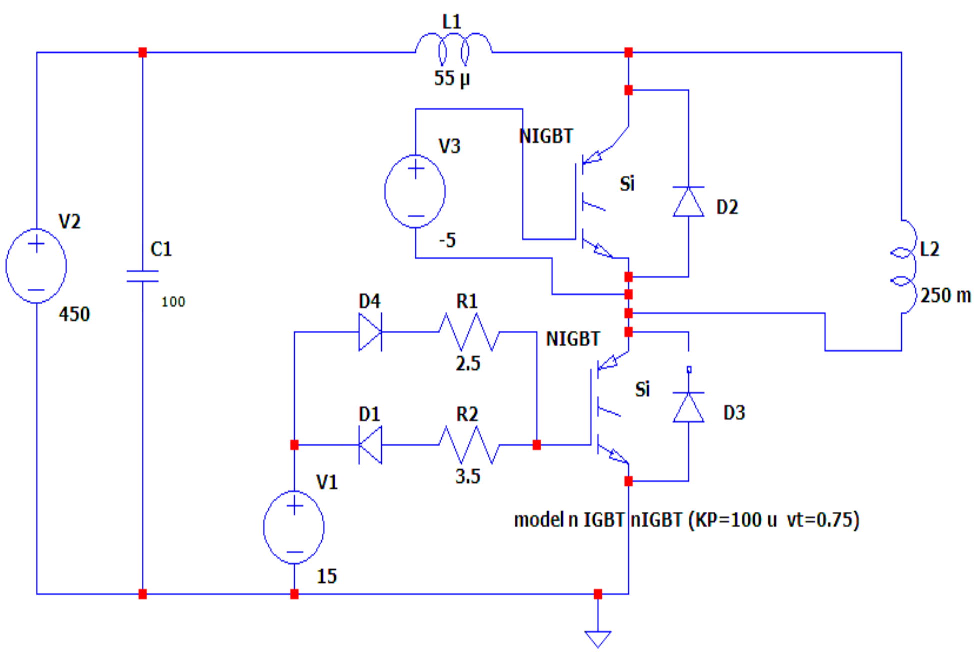

Figure 3 (a). Double-Pulse Test Arrangement

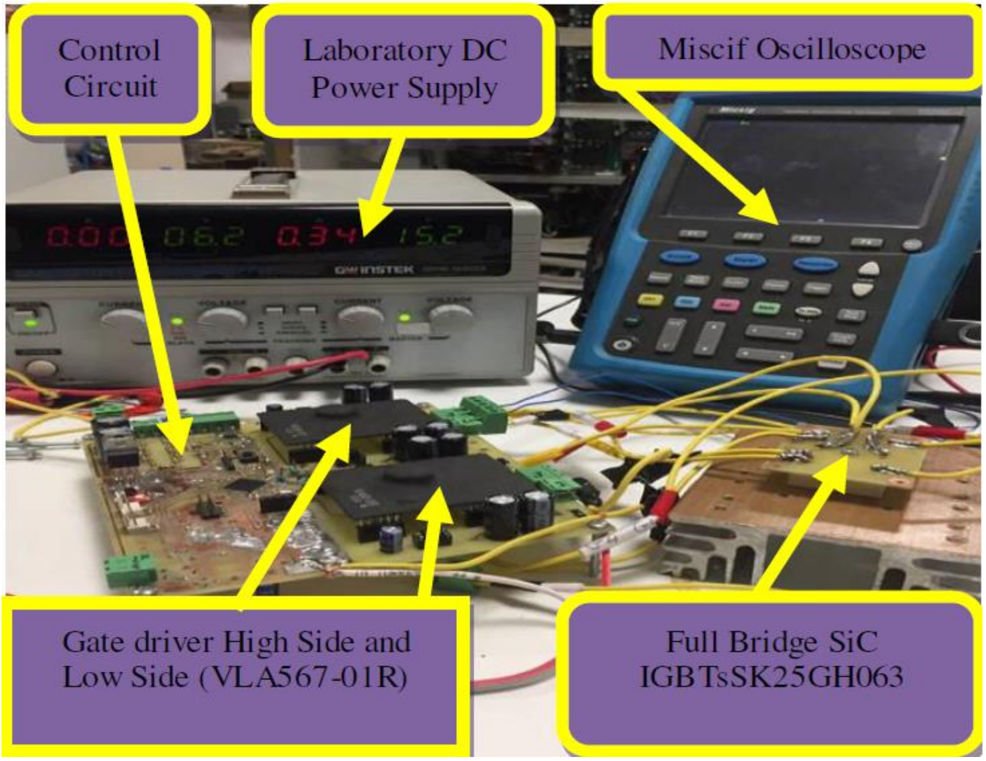

Figure 3(b). Implemented Circuit for SiC-IGBT Switches

4.1.1. Switching Characteristics and Switching Losses

At 100 Volt DC input voltages, a DPT was utilized to analyze the turn on characteristics of the SiC.IGBT and Si.IGBT In order to achieve the quickest switching, the original external gate resistances were utilized. In each experiment, the gate terminals of both switches had positive bias voltages of +15 V and negative bias voltages of -5 V. The switching losses of both transistors can be calculated using the oscilloscope's integration feature. Figure 4 shows the characteristics of the Si.IGBT experiment during turn off and turn on, whereas Figure 5 shows the characteristics of the SiC.IGBT experiment during turn off and turn on. Due to stray inductance in the test circuit, the turn off transient happened very quickly, causing a considerable voltage overshoot and prolonged ringing. It was also evident that raising the collector current caused the voltage to ring and overshoot. Table 2 shows the values for the Si.IGBT and SiC.IGBT turn on and turn off value.

Table 2. DPT experiment comparison of Si.IGBT and SiC.IGBT turn off and turn on times

Turn off and Turn on	SiC.IGBT	Si.IGBT	Load
	Input Voltage (100 Volts)	Input Voltage (100 Volts)	RL-Loads
Voltage Fall time	58 3ns	657 ns	3.8 A
Voltage Rise time	89 ns	396 ns	3.8 A

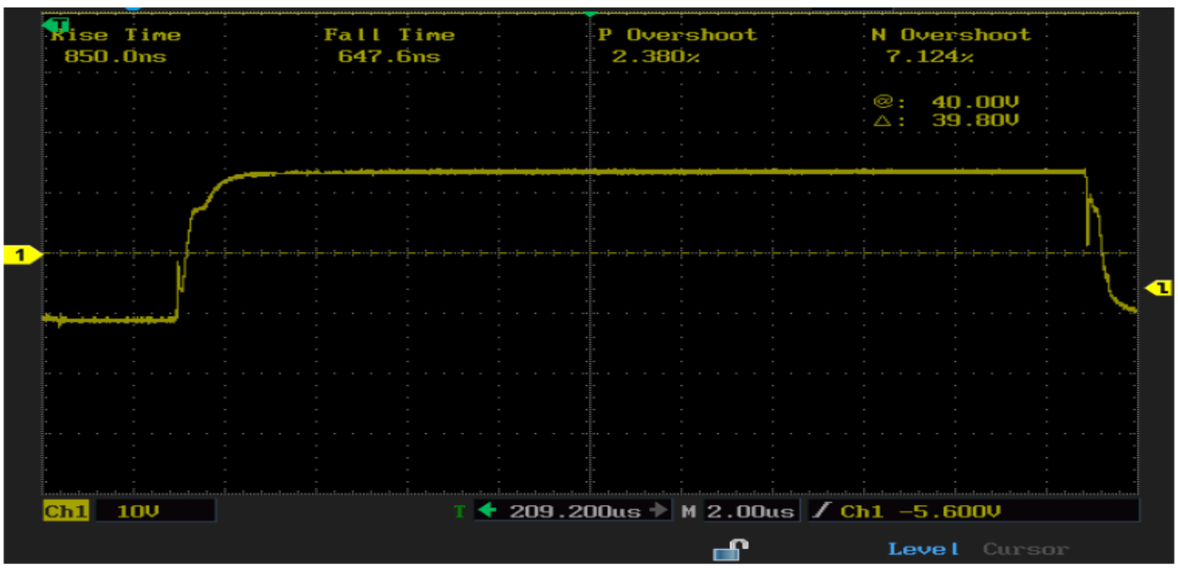

Figure 4. Switching waveforms (Si−IGBT- DPT experiment)

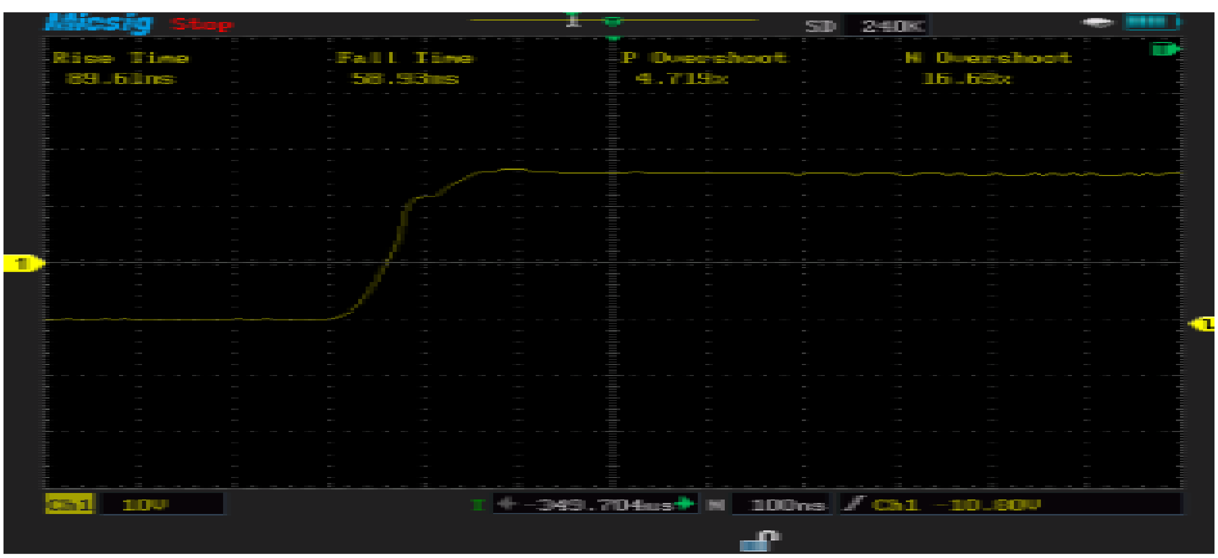

Figure 5. Switching waveforms (SiC−IGBT- DPT experiment)

4.2. PV Inverter Experiment

This study used a three-phase inverter design to measure a Si.IGBTs modules (1200 V/150 A). They are made up of gate driver, IGBT fuses (80A), inverter controller (DsPic-30F4011), output filter capacitor, IGBT switches (CM150DY-24), and gate capacitor. Figure 6 displays the parts of the TPVI. The TPVI is made up of two stages. A rectifier is used in the first stage as a DC to provide the required DC power, and an inverter is used in the latter stage. At the same frequency, it converts DC power to AC. The TPVI requirements are shown in Table 3.

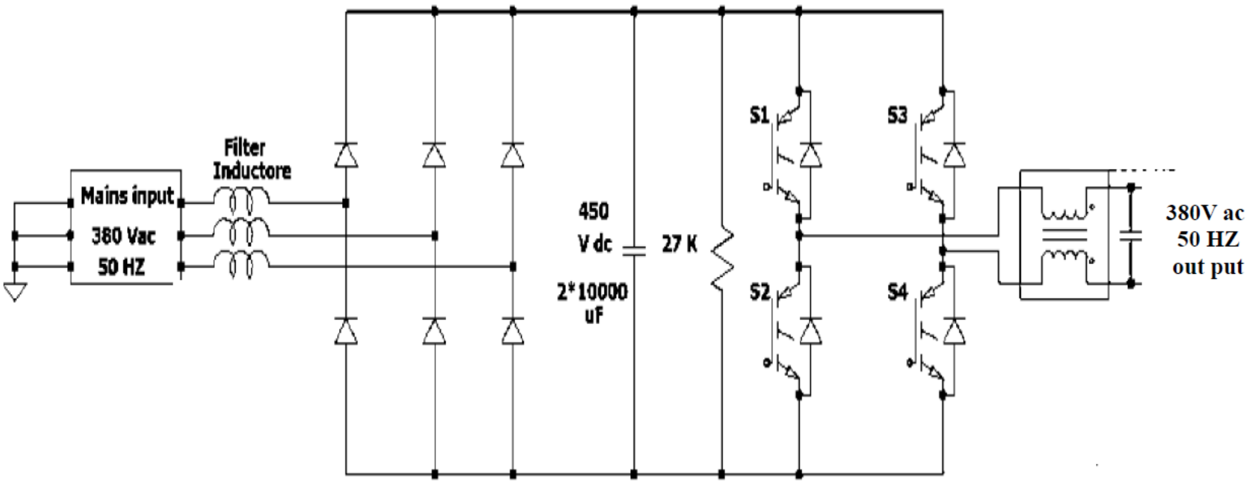

Figure 6. **(a).** System diagram of single phase for TPVI.

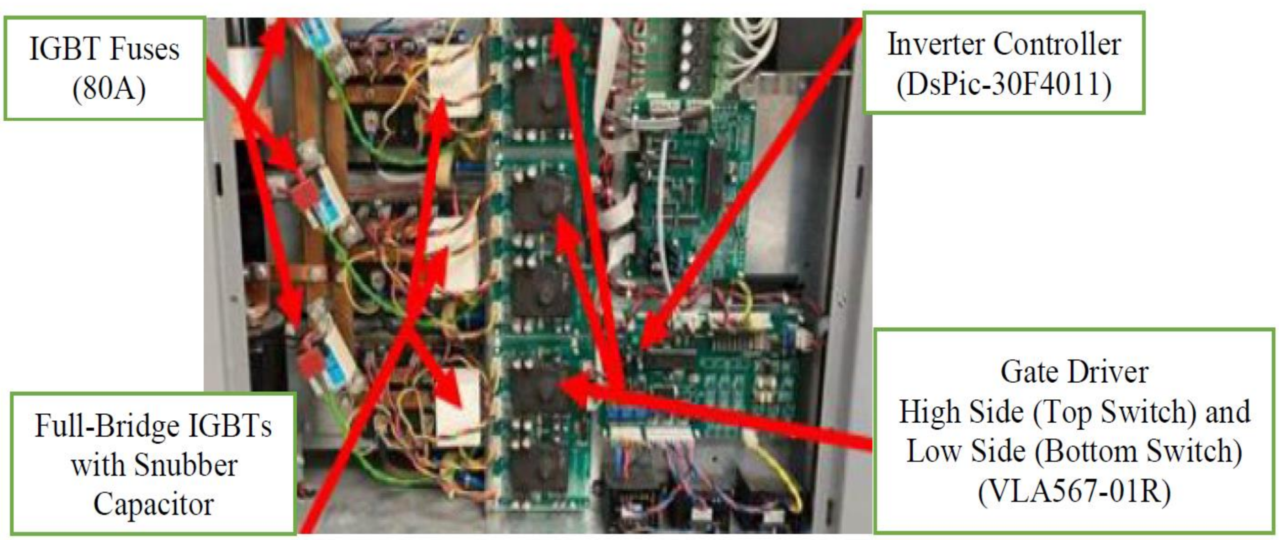

Figure 6. **(b)**. Three-phase inverter cabinet's electrical equivalent

Table 3. TPVI Cabinet Specifications.

MODEL	**Specification**
Input voltage	450 VDC (3-phase)
Output voltage	380 VAC (3-phase), stage
Maximum power	10kVA
frequency of input	50 Hz
frequency of Output	50Hz
DC current input	85 A
A DC bus	450VDC
Output transformer	transformer for galvanic isolation
Microcontroller	DsPIC30F4011 Microprocessor

4.2.1. Switching Characteristics and Switching Losses

This study includes measurements of switching timings, overshoot voltage, overshoot current, with RL load. A portable multipurpose oscilloscope from MICsig (200 MHZ), a clamp meter from Hantek (UT201), and a multimeter from Fluke (115 TRUE RMS) were used to analyze the characteristics of voltage and current. In order to demonstrate the benefits of the Si.IGBTs devices in terms of high frequency and high efficiency, experimental measurements of the turn off and turn on waveforms from the top and bottom sides were made. This experiment also measures the switching durations. Figure 7 displays the voltage rise time (296 ns) and voltage fall time (657 ns), with respective N-Over Shoot values of 11.5% and 2.2%. Additionally, it shows how switches turn on and off. The values for the Si.IGBT turn off and turn on values are displayed in Table 4.

Table 4. TPVI experiment comparison of Si.IGBT and SiC.IGBT turn off and turn on times

Turn off and Turn on	Si.IGBT	Load
	Input Voltage (100 Volts)	RL-Loads
Voltage Fall time	657 ns	3.8 A
Voltage Rise time	296 ns	3.8 A

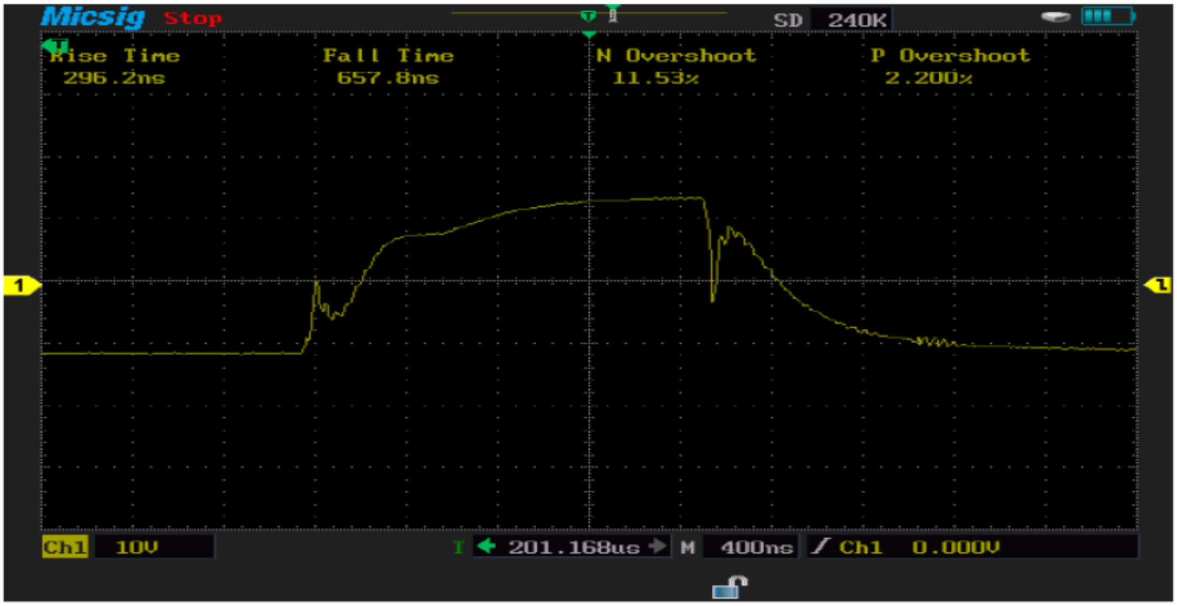

Figure 7. Three-phase inverter experiment using Si.IGBT transistors.

4.3. Total Switching Power Losses

The switching power losses of a high frequency switching system can be assessed using a three-phase inverter based on SiC.IGBT and Si.IGBT. It is feasible to analyze the turn on and turn off transients of a transistor in a three-phase inverter at a specific collector to emitter voltage and collector current. To calculate the power loss ($p_{T,loss}$), multiply the collector current by the collector to emitter voltage [18].

Power Loss ($p_{T,loss}$), $= i_c\ (t) * V_{ce}\ (t)$...(4.1)

Where i_c is the switching transistor's collector current and v_{ce} is the voltage between the collector and emitter.

4.3.1. Power Losses During Conduction

When a transistor is turned on, conduction power losses occur because of the transistor's on state collector to emitter resistance. Conduction power losses may be calculated by :

$$P_{T,Cond}\ (t) = R_{ce(on)}\ (t) * \ i_c^2\ \ (t)$$ ....(4.2)

Where $R_{ce(on)}$:Total the collector to emitter on resistance.

4.3.2. Losses on Switching on Average

When a three-phase inverter component is switched from off to on, switching losses take place. The collector current and collector to emitter voltage will both be greater than zero and will momentarily overlap during a switching transient. Power dissipation occurs in the IGBT as a result of overall power losses that are equal to collector current(i_c) times collector to emitter voltage (V_{ce}). Switching losses are a result of both transistor turn on and turn off switching. The Three phase inverter's energy losses $E_{T,on}$ and $E_{T,off}$ can be determined using the oscilloscope's integration feature. IGBT power dissipation occurs as a result of power loss $P_{T\,loss}=V_{ce} * i_c$. The total switching power loss ($P_{T,sw}$) in the IGBT transistor is:

$$P_{T\ sw} = \frac{1}{\pi} * f_{sw}\ (E_{T\ on}+E_{T\ off})\text{......}(4 . 3)$$

4.3.3. Total Power Output

The output power is obtained by multiplying the voltage at the load by the load current.

$$P_{out} = 3 * V_{load} * I_{load} = 3*m*\frac{V_{DC}}{2\sqrt{2}} * \frac{i_{load}}{\sqrt{2}}\text{......}(4 . 4)$$

4.3.4. Total Losses in Power

The total losses of the conduction pulse and switching losses are used to calculate the three phase inverter's conduction and switching losses.

$$P_{T,tot} = P_{T,Cond} + P_{T,sw}\text{......}(4 . 5)$$

4.3.5. Overall Losses

The overall losses of a three phase PV inverter, are determined by multiplying the number of switches by the total of the conduction losses.

$$P_{loss}=6*P_{T,tot}\text{......}(4.6)$$

4.3.6. Total Effectiveness

The power three phase PV inverter's overall efficiency is calculated by dividing the total power by the total power pulse.

$$\eta =\frac{P_{out}}{P_{out}+P_{loss}}\text{......}(4.7)$$

5. Discussion

The DPT with SiC.IGBT and Si.IGBT is utilized in this work to assess the switching characteristics while , the TPVI based on Si-IGBT is utilized in this study to assess the switching characteristics. The effectiveness of their operation under resistive and RL loads was assessed. The DPT based Si-IGBT's voltage fall time is 657 ns and its voltage rise time is 396 ns, compared to the SiC-IGBT's voltage fall time and voltage rise time of 58 ns and 89ns, respectively. The TPVI based Si-IGBT's voltage fall time is 657 ns and its voltage rise time is 296 ns. Consequently. These findings indicated that SiC.IGBT had a lower switching energy loss , and more larger oscillations , and switched off more quickly than Si-IGBT modules , It is clear that the SiC-IGBT is significantly more efficient. Review articles on three phase inverter systems are evaluated in based on semiconductor transistors and modulation methods. Several of these works used Si.MOSFET [19–20–21–22].

It was found that SiC-IGBT was not used for three phase PV inverters. Experimentally, DPT based on Si-IGBT efficiency was 77%, whereas SiC-IGBT efficiency was increased to 95%. The TPVI system based on Si-IGBT has an 86% efficiency. In this article, TPVI based on Si-IGBT switches are utilized; however, the following article will use SiC-IGBT switches.

6. Conclusion

In this work, it was demonstrated that employing SiC-IGBTs in TPVI systems might result in an increase in efficiency through the execution of practical experimental tests. The objective of this work was to construct and test TPVI that would deliver maximum efficiency with pure sinusoidal AC power. In order to do this, two different experimental setups were examined.

The Si.IGBT transistors with DPT experiment was evaluated in the first experimental study, and efficiency findings for the system were obtained, while the SiC.IGBT transistors with DPT experiment was developed and constructed for the same experimental study. The TPVI with Si.IGBTs switches alone has been developed to assess Si.IGBT performance. The SiC.IGBT with TPVI switches will be implemented and tested in the next article.

The operational capabilities of SiC.IGBT and Si.IGBT devices were examine and compared by the developed DPT experimental research. The TPVI system was meant to be utilized with the second experiment system. The operational characteristics of the TPVI based on Si.IGBT modules were examined. The switching performance and efficiency of Si.IGBT based systems were thoroughly assessed. Comparing the hard switching behavior of SiC.IGBTs and Si.IGBTs switches under the same layout and identical operating conditions. The impacts of switching timings (rise time and fall time), collector emitter voltage, gate to emitter voltage, positive and negative overshoot, and switching characteristics were explained in this paper. The SiC.IGBT's voltage fall time was quicker than the Si.IGBT's, as previously observed in the tables and figures, leading to a shorter overall switching time. The SiC.IGBT has a faster switching rate and significantly less loss than the Si.IGBT. The efficiency of SiC.IGBT modules was found to be higher than that of Si.IGBTs in the DPT. The analysis shows that DPT can be created at 20 kHz with Si.IGBT efficiency of 77%, whereas SiC.IGBT can be made at the same switching frequency with SiC.IGBT efficiency of 95%. The Si.IGBT-based TPVI system has an 86% efficiency. To increase efficiency, the SiC transistor could perhaps replace the Si transistor. According to the results of the experimental tests, it can be seen that SiC.IGBTs may increase efficiency in conventional TPVI systems.

Author Contribution: I.A.S.A. Methodology, validation, software, analytical procedure, research, resources, curation of data, writing (original draft), writing (review and editing), visualization, management of projects, financing acquisition, preparation, investigation and supervision.

Funding: There was no external support for this study.

Conflicts of Interest: There is no conflict of interest for the author.

References

1 . W. G. Homeyer. Lupan, S.P., Walia, P.S., and Bowles, E.E. Power Converter (MEA Application). IECEC-97 Thirty-Second Intersociety Energy Conversion Engineering Conference Proceedings, 27 July–1, Honolulu, Hawaii, USA (Cat. No. 97CH6203) August 1997.

2 . Immanuel, V.D.; Burgos, R.; Boroyevich; Lai, R.; Wang, F.; Ning, P.; Zhang, D.; Jiang, D.; Karimi, K.J. Power Density Converters.; 4, 4–12 IEEE Industrial Electron Magazine2010.

3 . Yin, S.; Sakanova, A.; Liu, Y.; Liu, Y.; Kai, M.; et al. Nawawi, A.; Simanjorang, R.; Gajanayake, C.J.; Gupta, A.K.; Tong, C.F. high power density inverters for (MEA Application). 53, 1168–1176 IEEE Trans. Ind. Appl.2016 .

4 . Yoshida, T., Yokakohara, Y., Otake, H., Evans, T.M., Tsuruya, M., and K. Nakahara. DC-DC Converters with SiC MOSFET, 63, 2103-2110 IEEE Trans. Ind. Electron , 2015.

5 . Roux, N., Cougo, B., Sathler, H., Riva, R., Dos Santos, V., and Sareni, B. SiC Modules - integrated capacitors (MEA Application). 36, 8230–8242 IEEE Trans. Power Electron. 2021.

6 . Kawai, F.; Ajioka, M.; Nagao, K.; and Hamada, K. SiC Power Devices Technologies., 62, 278–285 IEEE Trans. Electron, Devices 2014.
7 . Huang, A.Q.; Wang, F.; Song, X.; Ni, X.; Ryu, S.H.; Grider, D.; Schupbach, M.; Palmour, J. Dynamic Performance Characterization (15 kV SiC MOSFETs with 15 kV SiCs nIGBTs). Page numbers 229–232 in Proceedings of the IEEE 27th International Symposium on Power Semiconductor Devices & IC's (ISPSD), Hong Kong, China, 10–14 May (2015).
8 . Mainali, Kadavelugu, Patel, Madhusoodhanan, Tripathi, Hatua, Bhattacharya, Ryu, Grider, D., and S. Leslie. power converter design (15 kV SiC N-IGBTs).;Charlotte, North Carolina, USA; Proceedings of the IEEE Conference on Applied Power Electronics Conference and Exposition; pp. 1396–1403. (2015).
9 . Yonezawa, Y., Mizushima, T., Matsunaga, S., Iizuka, Y., and Yamaguchi, H. dynamic behavior of a medium voltage n channel SiC-IGBT (300 kv-µs). IEEE Trans. Industrial Appl., 54, 3558–3565 (2018).
10 . Kusetogullari, H., Kivrak, S., and Karabulut, M. outdoor performance assessment of new @ old PV. J. Photoenergy 2020, 8866412, 2020.
11. T. Celik and H. Kusetogullari. Solars Power (Speed Violation Detection)., 57, 3216–3227, IEEE Trans. Ind. Electron ,(2009).
12 . Remus Teodorescu, Aalborg University, Denmark. Marco Liserre, Politecnico di Bari, Italy. Pedro Rodr´ıguez, Technical University of Catalonia, Spain..GRID Converters for PV and wind power systems.This edition first published C 2011, John Wiley & Sons, Ltd (2011).
13 . IEC Standard 61727, Characteristic of the Utility Interface for Photovoltaic (PV) Systems, 2002.
14 . A. Kadavelugu and S. Bhattacharya, “Design (gate driver for 15 kV SiC IGBT) ”in Proc. Appl. Power Electron. Conf. Expo. (APEC), Mar., pp. 1494–1501(2014).
15 . Data sheet . Hybrid IC IGBT Gate Driver + DC/DC Converter Powerex, Inc.,Lane, Youngwood, Pennsylvaniawww.pwrx.com http : // www .pwrx .com / pwrx / docs/VLA567-01R.pdf.
16 . N. Mohan , T. M. Undeland, and W. P. Robbins. Converter, Application. Wiley, Hoboken, New Jersey, USA,; 3rd ed,(2003).
17 . Shi, C.; Zhang, C.; Zhang, J.; Yuan, X.; Zhang, Y.; Zhang, L. high power SiC mosfet comparison to Si igbts modules.; 34; 1181–1196; IEEE Trans. Power Electron (2019).
18 . I . Abdalgader , S. Kivrak and T Özer, Comparison (SiC-IGBT and Si-IGBT) in Inverter for aircraft applications, yildirim beyazit university, ankara 06000, turkey2022.
19 . Boroyevich, D.; Ngo, K.D.; Mattavelli, P.; Rajashekara, K.; Yao, Y.; Chen, Z. SiC mosfet (high temperature, high frequency applications). 29, 2307-2320 IEEE Trans. Power Electron ,(2013).
20 . Guo, W.; Doran, P.; Perdikakis, W.; Sheets, A.; Scott, M. EMI Analysis (high power silicon carbide) two level inverter. The sixth IEEE Workshop on Wide Bandgap Power Devices and Applications , atlanta, georgia, usa ,(2018).
21 . Mahajan S.B ; Pachagade R.M ; Badave S.M ; Pandav k.M ; Sanjeevikumar P. three phase inverter (2.4 kW) for aircraft application. Springer, Singapore power systems and energy management; 2018 .
22 . Amit gupta, chandana gajanayake, chen jiawei, lee meng yeong, Wen Changyun, three phase four leg inversion power supply for (MEA). ieee conference(ICIEA), Zealand,(2015).